Journal of Medicinal Chemistry

Article

pubs.acs.org/jmc

Identification of Small Molecule Inhibitors of Amyloid β-Induced Neuronal Apoptosis Acting through the Imidazoline I_2 Receptor

Marisol Montolio,[†] Elisabet Gregori-Puigjané,[‡] David Pineda,[†] Jordi Mestres,*[,‡] and Pilar Navarro*[,†]

[†]Cancer Research Program and [‡]Biomedical Informatics Program, IMIM—Hospital del Mar Research Institute and University Pompeu Fabra, Parc de Recerca Biomèdica (PRBB), Doctor Aiguader 88, 08003 Barcelona, Catalonia, Spain

Supporting Information

ABSTRACT: Aberrant activation of signaling pathways plays a pivotal role in central nervous system disorders, such as Alzheimer's disease (AD). Using a combination of virtual screening and experimental testing, novel small molecule inhibitors of tPA-mediated extracellular signal-regulated kinase (Erk)1/2 activation were identified that provide higher levels of neuroprotection from Aβ-induced apoptosis than Memantine, the most recently FDA-approved drug for AD treatment. Subsequent target deconvolution efforts revealed that they all share low micromolar affinity for the imidazoline I_2 receptor, while being devoid of any significant affinity to a list of AD-relevant targets, including the *N*-methyl-D-aspartate receptor (NMDAR), acetylcholinesterase (AChE), and monoamine oxidase B (MAO-B). Targeting the imidazoline I_2 receptor emerges as a new mechanism of action to inhibit tPA-induced signaling in neurons for the treatment of AD and other neurodegenerative diseases.

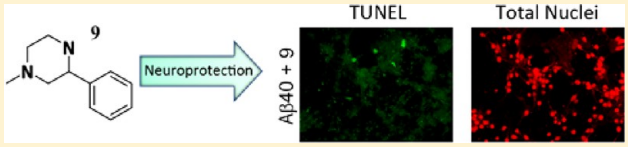

INTRODUCTION

Cell signaling pathways are essential to regulate cellular activity. They are responsible for key cell functions such as growth, metabolism, cytoskeletal regulation, adhesion, translational control, DNA damage, and apoptosis. Well-orchestrated activation of cell signaling pathways is required during cell development and differentiation as well as for the maintenance of cellular homeostasis. Among the large number of intracellular signaling pathways, the extracellular signal-regulated kinase (Erk) is one of the first and best-characterized signal transduction networks. The Erk1/2 kinases are serine/threonine kinases that belong to the mitogen-activated protein kinase (MAPK) superfamily of signaling proteins, and they integrate cellular signals in response to a variety of stimuli that affect cell proliferation, differentiation, and survival. Altered activation of Erk signaling pathway results in cell dysfunctions that have been found to be linked to severe pathologies such as cancer or neurological disorders.[1,2]

In the central nervous system (CNS), induction of Erk cascade is critical for learning and memory,[3] and aberrant Erk activation has been particularly reported in the pathogenesis of Alzheimer's disease (AD),[4−6] a devastating CNS pathology characterized by progressive neuronal loss accompanied by cognitive decline and dementia.[7] Amyloid-β (Aβ) is recognized to play a central role in the synaptic dysfunction and neurodegeneration linked to AD,[8] and its accumulation is known to induce sustained Erk activation both in vitro[5,9] and in vivo,[5,10] ultimately leading to neuronal death. However, the molecular mechanisms underlying Erk stimulation by Aβ are not yet completely understood. In this respect, it was previously reported that tissue plasminogen activator (tPA) is involved in this event.[6] Even though tPA is mainly known as a fibrinolytic agent in the conversion of plasminogen into plasmin,[11] a recent study showed that it mediates Aβ-induced apoptosis through a rapid and sustained catalytic-independent activation of the Erk1/2 signal transduction pathway.[6] Indeed, Aβ treatment after pharmacological inhibition of tPA or in primary neurons obtained from tPA−/− mice failed to induce Erk activation and neuronal apoptosis,[6] indicating that inhibition of tPA-induced signaling in neurons could represent a novel approach to prevent Aβ-mediated neurotoxicity and thus become a valuable strategy in the treatment of AD.

On this basis, the present study aims at probing the link between tPA-mediated Erk1/2 activation and Aβ-induced apoptosis with small molecules as a means to identify protein targets that could play a key role in managing this connection. Using MK-801, a previous work confirmed that the NMDA receptor (NMDAR) is one of those targets.[6] Through the identification of novel small molecules that inhibit the Erk1/2 signaling pathway and protect against Aβ neurotoxicity, this study reveals that the imidazoline I_2 receptor is another one of those targets, paving the way to novel strategies to AD pathogenesis.

RESULTS

Novel Inhibitors of tPA-Induced Erk1/2 Activation. Identification of small molecules inhibiting tPA-induced Erk1/2 activation was performed in primary cultures of mouse hippocampal neurons, as this cellular system can mimic the in vivo situation during AD, where hippocampus is one of the most affected regions. Given the limited capacity of an experimental assay involving the use of primary cultures, we had to revert to computational approaches to prioritize a small

Received: July 19, 2012
Published: October 25, 2012

   dx.doi.org/10.1021/jm301055g | J. Med. Chem. 2012, 55, 9838−9846

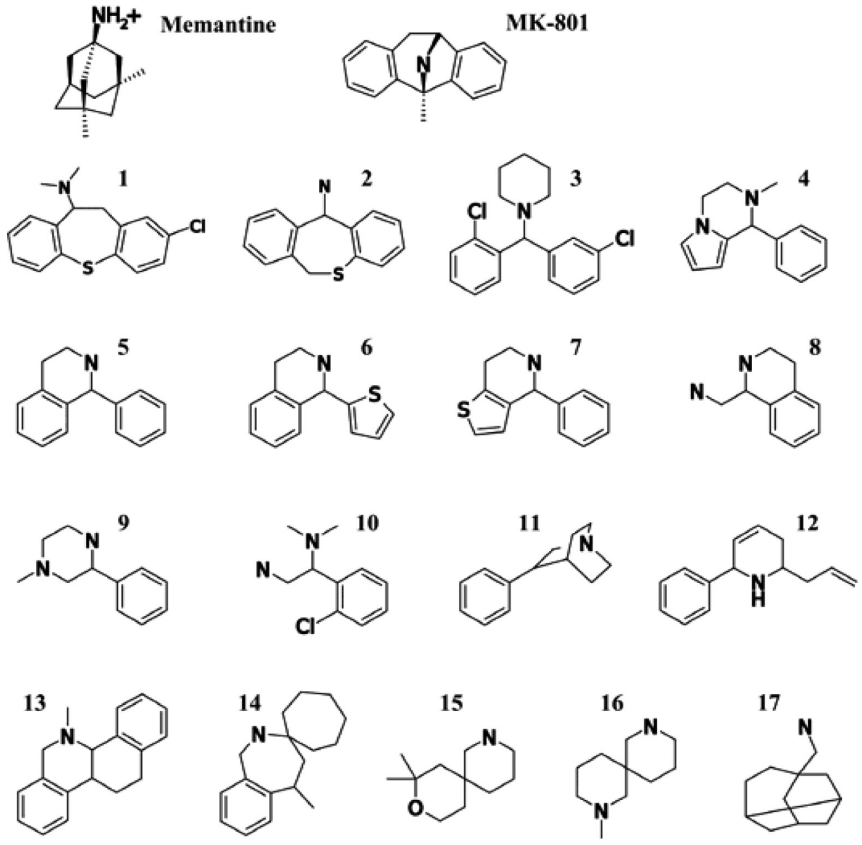

Figure 1. Chemical structures of the two reference compounds, Memantine and MK-801, and the 17 compounds purchased from commercial providers and analyzed in this work.

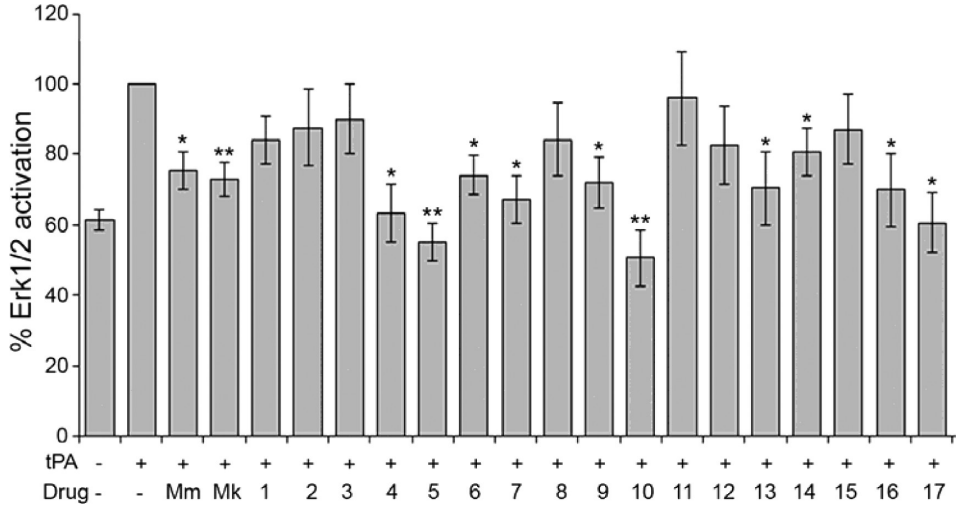

Figure 2. Inhibition of tPA-induced neuronal Erk1/2 activation. Primary mouse hippocampal neurons were treated with medium alone (−, negative control), tPA (20 μg/mL, 1 h), or tPA in the presence of Memantine, MK-801, or molecule **1**−**17** at 30 μM. Phospho- (activated) and total-Erk1/2 were detected by ELISA. The graph corresponds to the quantification of Erk1/2 activation with respect to tPA levels, normalized to the total amount of Erk1/2. Statistical analyses were performed with a two-tailed Student's test (n = 4), and data are mean values ± SEMs. *$P \leq 0.05$ and ** $P \leq 0.001$, as compared to tPA conditions.

number of selected compounds that would ultimately go into testing. As mentioned above, a previous study showed that MK-801, a high-affinity noncompetitive NMDAR antagonist,[12] was able to abolish completely the activation of the Erk1/2 signaling pathway by tPA.[6] The same effect was later observed with Memantine (vide infra), a low-affinity noncompetitive NMDAR antagonist[13] currently used widely as first-line treatment of AD. Because information on two small molecule inhibitors of tPA-mediated Erk1/2 activation was available, similarity-based virtual screening emerged as an obvious option to prioritize compounds for experimental testing. In this respect, we used a similarity approach based on Shannon entropy descriptors (SHED)[14] derived from topological feature distributions that were successfully applied recently in the

dx.doi.org/10.1021/jm301055g | J. Med. Chem. 2012, 55, 9838−9846

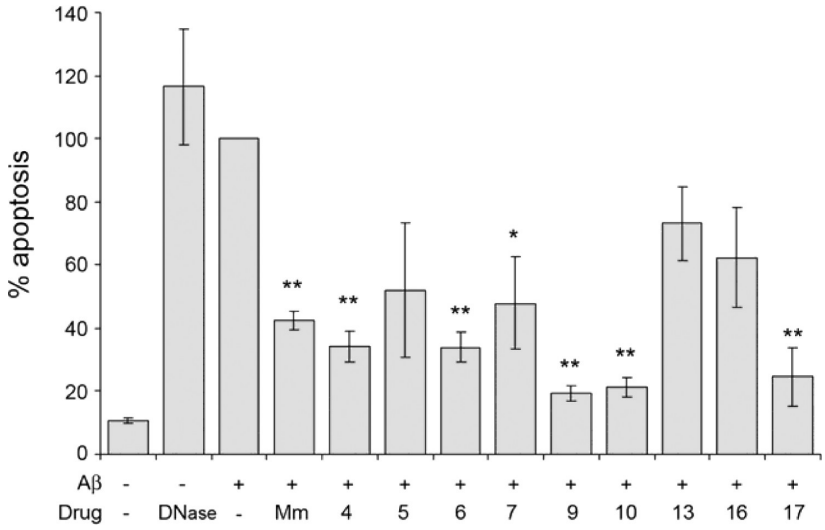

Figure 3. Inhibition of Aβ-induced neuronal apoptosis. Primary mouse hippocampal neurons were treated with Aβ (20 μM, 72 h) alone or in the presence of Memantine or different molecules (**4**–**7**, **9**, **10**, **13**, **16**, or **17**) at 30 μM. Neuronal apoptosis was detected by TUNEL staining. The graph represents the percentage of apoptotic cells relative to the total number of nuclei and referred to Aβ conditions (100%). Neurons treated with medium alone (−) or DNase were used as negative and positive controls, respectively. Statistical analyses were performed with a two-tailed Student's test (n = 4), and data are mean values ± SEMs. *$P \leq 0.05$ and ** $P \leq 0.001$, as compared to Aβ conditions.

identification of novel compounds that reactivate latent HIV-1.[15]

Accordingly, MK-801 and Memantine were taken as reference structures (Figure 1) from which similar compounds were searched in a commercial chemical catalogue composed of over 2 million compounds. A total of 1758 compounds were retrieved under a SHED Euclidean distance cutoff of 1.5. Of those, 1453 and 305 were found to have structures with topological pharmacophoric features distributed similarly to MK-801 and Memantine, respectively (Table S1 in the Supporting Information). To reduce the number of compounds further, a scaffold analysis was performed by extracting the atomic frameworks of all molecules using an internally developed chemical graph identifier:[16] Four hundred forty-six scaffolds were identified, and a representative molecule of each scaffold was selected. Finally, a cost filter was applied to those 446 molecules. After visual inspection, 17 cost-effective molecules with scaffold topologies strictly different from MK-801 and Memantine were prioritized for purchase from commercial providers (Table S2 in the Supporting Information). The structures of these molecules are collected in Figure 1, of which 14 (molecules **1**–**14**) and 3 (molecules **15**–**17**) come from the sets of molecules having pharmacophoric distributions similar to MK-801 and Memantine, respectively.

The 17 molecules selected were experimentally tested for their capacity to inhibit Erk1/2 activation induced by tPA treatment of hippocampal neurons as a primary test for the more elaborate testing of Aβ-induced apoptosis. Detection of activated Erk1/2 was performed by ELISA using an antibody specific for phosphorylated Erk1/2, and values were normalized using an antibody against total Erk1/2 (Figure 2). The lower and upper Erk1/2 activation limits were established with the basal level observed with untreated cultures and its stimulation in the presence of tPA, respectively. Memantine and MK-801 were taken as positive controls, and their levels of inhibition of Erk1/2 activation were used as criteria for the identification of novel bioactive molecules. As can be observed, 10 molecules showed statistically significant inhibition of Erk1/2 activation by tPA, and nine of them (53% of all molecules purchased and tested) showed similar (**6**, **9**, **13**, and **16**) or enhanced (**4**, **5**, **7**, **10**, and **17**) levels of inhibition of Erk1/2 as compared to those obtained with Memantine or MK-801.

All nine bioactive molecules identified have scaffold structures that are strictly different from the ones present in the two reference compounds (Figure 1). In terms of pharmacophoric distributions, they can be broadly organized in three clusters. The largest pharmacophoric cluster, cluster I, is composed of five out of the nine bioactive molecules (**4**, **5**, **6**, **7**, and **13**), the structures of which are characterized by the presence of two aromatic centers, each of them being two bonds away from a positively charged amine, the essential pharmacophoric signature of MK-801. A second pharmacophoric cluster, cluster II, is defined by two molecules (**9** and **10**) that differ from the structures present in cluster I by the fact that one of the aromatic centers is substituted by a second positively charged amine, a bioisosteric replacement used commonly in medicinal chemistry. The final cluster, cluster III, contains the two remaining bioactive molecules (**16** and **17**) that retain the main pharmacophoric features present in the structure of Memantine. These 11 molecules will be considered for further testing for their ability to inhibit Aβ-induced neuronal apoptosis.

Inhibition of Aβ-Induced Neuronal Apoptosis. It has been previously reported that Aβ induces neuronal toxicity through Erk1/2 activation[5,9,17] and that these effects are mediated by tPA.[6] Accordingly, the next step was to test the nine molecules identified as inhibitors of tPA-mediated Erk1/2 activation for their neuroprotective effects against Aβ-induced apoptosis. Primary cultures of mouse hippocampal neurons were treated with aggregated Aβ alone (taken as positive control) or in the presence of each bioactive molecule, and apoptosis was quantitatively assessed by measuring the number of positive nuclei detected by TUNEL labeling. The percentages of Aβ-induced apoptosis achieved in the presence of the different small molecules in comparison to values observed after single Aβ treatment (normalized to 100%) are presented in Figure 3. Untreated cells were used to provide the basal level of apoptosis in primary cultures (10.5 ± 0.8%).

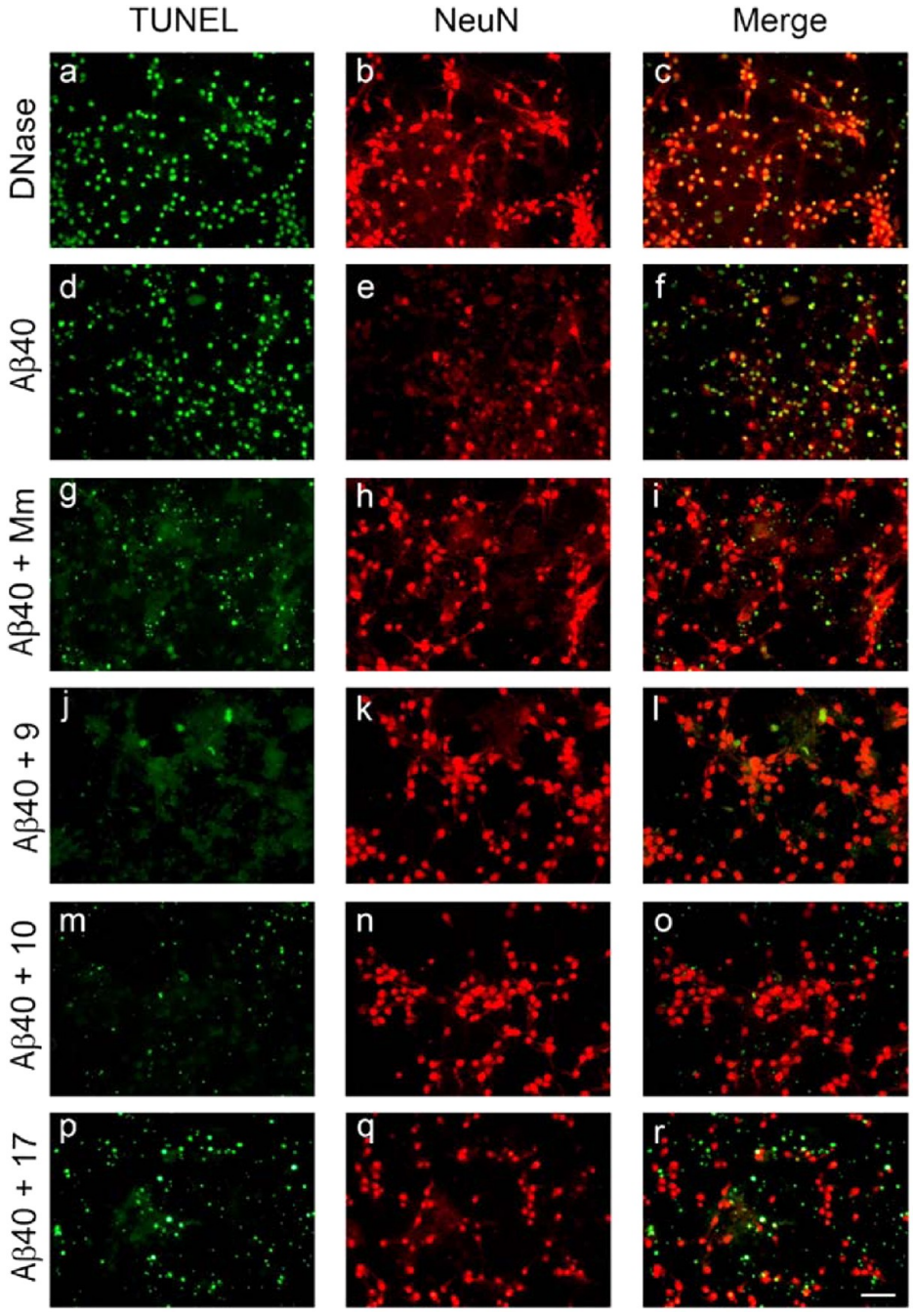

Figure 4. Molecules **9**, **10**, and **17** show neuroprotection against Aβ toxicity. Primary mouse hippocampal neurons were treated with Aβ (20 μM, 72 h) (a–c) or Aβ in the presence of Memantine or different molecules (**9**, **10**, and **17**). Cells were analyzed by immunofluorescence microscopy to detect DNA fragmentation (TUNEL, green), total neuronal nuclei (NeuN, red), and overlay (merge). Treatment with DNase was used as a positive control. Bar, 50 μm.

Neurons were also treated with DNase as an additional positive control of apoptosis (116.4 ± 18.3%). Finally, the reduction of cellular apoptosis observed when neurons were preincubated with Memantine prior to Aβ addition (42.3 ± 2.7%) served to establish the target criteria for apoptotic protection to be achieved by novel neuroprotective small molecules.

The results show that out of the nine molecules selected in the first round of Erk-inhibition ELISA screening, five of them provided better levels of neuroprotection from Aβ-induced apoptosis than Memantine (**4**, **6**, **9**, **10**, and **17**); one also showed a significant decrease of Aβ-induced apoptosis (**7**), and another three were found to achieve only weak, not reaching statistical significance, apoptotic protection (**5**, **13**, and **16**). Accordingly, focus turned then into further characterizing the three molecules that showed the highest levels of neuroprotection from Aβ-induced apoptosis (**9**, **10**, and **17**). Figure 4 shows the efficiency of molecules **9**, **10**, and **17** to protect against apoptosis triggered by Aβ by double immunofluorescence of apoptotic nuclei (TUNEL, green) and total neuronal nuclei (NeuN, red), as well as the combined images (merge). Both DNase (Figure 4a–c) and Aβ (Figure 4d–f) treatments lead to extensive neuronal apoptosis, whereas pretreatment with Memantine (Figure 4g–i), **9** (Figure 4j–l), **10** (Figure 4m–o), or **17** (Figure 4p–r) rescue the Aβ pro-apoptotic

dx.doi.org/10.1021/jm301055g | J. Med. Chem. 2012, 55, 9838–9846

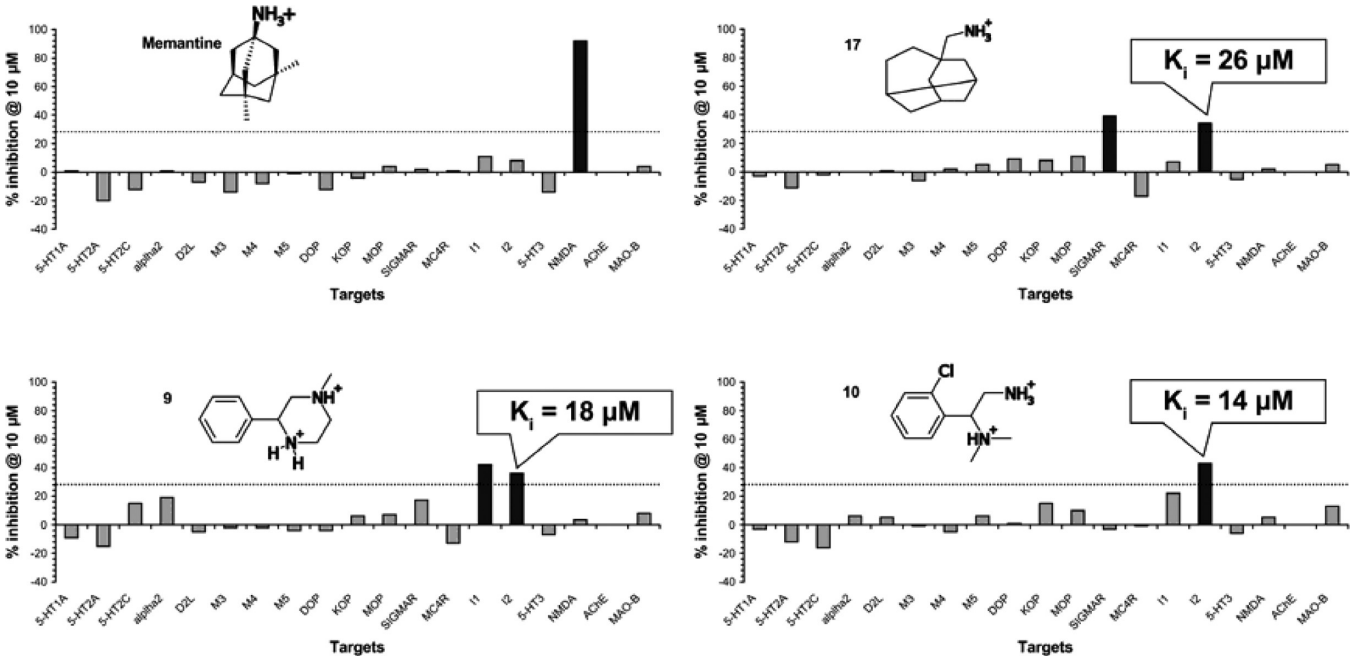

Figure 5. Single concentration in vitro profile (% inhibition at 10 mM) of Memantine and compounds **9**, **10**, and **17** across a list of 19 targets (see the text for target acronyms). Dose–response curves corresponding to the K_i values for the interaction with the imidazoline I_1 and I_2 receptors are provided in Figure S1 in the Supporting Information.

effects. Therefore, molecules **9**, **10**, and **17** represent novel chemical entities with clear enhanced protective effects against neuronal apoptosis.

Target Deconvolution. Because the novel neuroprotective molecules identified were originally selected from chemical providers by pharmacophoric feature similarity to NMDAR antagonists, our first assumption was to contemplate NMDAR as the obvious target for compounds **9**, **10**, and **17**. Accordingly, these three compounds were submitted for testing on radioligand binding assays for the four binding sites (agonist/glutamate, glycine, phencyclidine, and polyamine) reported to regulate NMDAR activity. Memantine and MK-801, as reference NMDAR antagonists, and compound **5**, as representative of the group of compounds retaining the essential pharmacophore features of MK-801 (vide supra), were also tested on the same four assays. The results, shown in Figure 5, confirmed a full binding affinity of Memantine (92% at 10 μM) and MK-801 (98% at 10 μM) for the phencyclidine site of the NMDAR and consistently revealed significant affinity on this assay also for compound **5** (69% at 10 μM). However, most surprisingly, compounds **9**, **10**, and **17** were found to be completely inactive in all NMDAR assays. We had then three compounds that showed significantly better neuroprotective effects than Memantine in an Aβ-induced apoptosis phenotypic assay (Figure 3), but unlike Memantine, they were not interacting with the phencyclidine site of the NMDAR. From a puristic standpoint, because these three compounds were selected based on their similarity to Memantine and MK-801, they would be considered false positives in the virtual screen. Therefore, a target deconvolution effort to identify the potential target(s) of those compounds was initiated. For the sake of clarity, this target identification is unrelated to the virtual screen and only makes sense in this particular setting that combines in silico and in vitro approaches.

To this aim, a screening panel of in vitro assays was defined to further extend the pharmacological profile of the compounds. A first set of 14 binding assays was selected on the basis of prior evidence of relevance to AD.[18] This included the serotonin 5-HT_{1A}, 5-HT_{2A}, and 5-HT_{2C} receptors, an unspecific α adrenoceptor type 2 (α2), the dopamine D2 receptor, the muscarinic M3, M4, and M5 receptors, the three δ-, κ-, and μ-opioid receptors (DOP, KOP, and MOP), the serotonin 5-HT3 ion channel, and the acetylcholinesterase (AChE) and monoamine oxidase type B (MAO-B) enzymes. In addition, similarity-based computational methods were recently applied to predict the likely protein targets of small molecules bioactive in phenotypic screens.[19] Accordingly, the previous selection was complemented with the results obtained from an in silico target profiling of compounds **9**, **10**, and **17** using a similarity-based approach that was recently validated both retrospectively, on its ability to predict the entire experimental interaction matrix between 13 antipsychotic drugs and 34 protein targets[20] and to identify cancer-relevant proteins in a target deconvolution study of selective cytotoxic compounds in tumor cells,[21] and prospectively, on its capacity to identify the correct targets for all molecules contained in a biologically orphan chemical library[22] and to anticipate the affinity profile of the muscle relaxant drug cyclobenzaprine.[23] Compound **9** was predicted to have affinity for the melanocortin 4 receptor (MC4R), and compound **17** was predicted to have affinity for the σ-1 receptor (SIGMAR) and nischarin. The latter is likely the I_1-imidazoline receptor,[24] and thus, the binding assays available for the imidazoline I_1 and I_2 receptors, in addition to MC4R and SIGMAR, were also included in the final list of targets to screen. In total, Memantine (as reference molecule) and compounds **9**, **10**, and **17** were profiled in vitro against a panel of 19 radioligand binding assays. The final results of this target fishing campaign are presented in Figure 5 as average percentages of inhibition of specific binding when tested with potent standard ligands for the respective targets (see the Experimental Section).

dx.doi.org/10.1021/jm301055g | J. Med. Chem. 2012, 55, 9838–9846

As can be observed, within the target space explored, Memantine shows a clear selective affinity profile for the phencyclidine site of the NMDAR. However, most interestingly, at least one target was identified for which each of the other three compounds shows average inhibition of binding above the threshold of 30% at 10 μM. In this respect, compound **17** has dual affinity for SIGMAR (39% at 10 μM) and I_2 (34% at 10 μM), as correctly anticipated from in silico target profiling; compound **9** shows also dual affinity but for the pair of I_1 (41% at 10 μM) and I_2 (36% at 10 μM) receptors, whereas compound **10** seems to interact mainly with I_2 (43% at 10 μM). Dose−response curves were determined to further confirm the affinities of compounds **9**, **10**, and **17** for the imidazoline receptors (Figure S1 in the Supporting Information). The strongest affinity was obtained for the interaction between compound **10** and I_1, with a pK_i value of 5.2 μM. The affinities between compounds **9**, **10**, and **17** and I_2 were comparatively weaker, with pK_i values of 18, 14, and 26 μM, respectively. In this regard, it is remarkable to confirm that all three compounds share low micromolar affinity for this common target: the imidazoline I_2 receptor.

DISCUSSION AND CONCLUSIONS

Compelling evidence has demonstrated a role for Erk1/2 activation in neurodegeneration,[2] although little information is available about the pharmacological use of Erk1/2 inhibitors in neurodegenerative diseases. In the present study, we have identified novel small molecules that efficiently inhibit neuronal Erk1/2 activation induced by tPA and display high levels of neuroprotection against amyloid toxicity, a key contributor to AD,[8] supporting a role for Erk1/2 inhibitors as novel therapeutic targets for AD treatment. Identification of the putative molecular target of the three most active neuroprotective molecules (**9**, **10**, and **17**) reveals a richness of genuinely different and novel mechanisms of action that all converge in the imidazoline I_2 receptor. Therefore, although we cannot rule out a synergistic effect of I_1 and σ-1 receptors in the action of compounds **9** and **17**, respectively, or of any other target outside the panel screened, the fact that all three compounds share a common binding to I_2 suggests that their neuroprotective effect is likely to be mediated by this receptor. Interestingly, imidazoline receptors have been previously shown to be up-regulated (30−36%) in brains of patients with AD,[25] suggesting that these receptors could be relevant targets for therapy.

Despite being in the low micromolar range, the affinities between compounds **9**, **10**, and **17** and I_2 receptors are biologically relevant under the compound concentrations used in all assays of this study (30 μM). Nonetheless, one ought to take into consideration that the I_2 affinity values obtained may vary depending on the particular labeled ligand, tissue, and species employed in the assay. For example, in our I_2 assay, [^{3}H]idazoxan (+1 μM yohimbine) was used as a labeled ligand in the rat cerebral cortex. However, it was recently reported that the affinity of CR4056 for I_2 receptor varied from 66% inhibition of specific binding when using [^{3}H]idazoxan (+1 μM yohimbine) as the labeled ligand in rat cerebral cortex (as in our assay) to 92% when [^{3}H]2-(2-benzofuranyl)-2-imidazoline) (2-BFI) was used as the labeled ligand in rat whole brain instead.[26] Moreover, we should take into account that the inhibition of binding receptor found in our assays could be mediated by direct binding of our hits to the identified targets or by other mechanisms, as allosteric modulation via non-radioliganded binding sites.

Characterization of the affinity profile of compounds **9**, **10**, and **17** across a set of 19 AD-relevant targets revealed that their mechanisms of action are unique as compared to those established for current AD drugs and other multitarget strategies proposed recently.[27−30] Essentially, apart from the low micromolar affinity identified for I_2 (**9**, **10**, and **17**), I_1 (**9**), and σ-1 (**17**) receptors, no significant affinity (<20% at 10 μM) is obtained for any of the other 16 AD-relevant targets screened, including classical AD targets such as MAO-B, AChE, and NMDAR, the latter two linked to FDA-approved AD drugs such as donepezil, galantamine, and rivastigmine, on one side, and Memantine, on the other side.[31] Thus, molecules **9**, **10**, and **17** exemplify that it is possible to achieve neuroprotective levels similar to or better than Memantine (Figure 3), through a NMDAR-independent mechanism of action that involves interacting with the I_2 receptor (Figure 5). Moreover, these three compounds also show unique characteristics in comparison to other imidazoline I_2 ligands previously reported with neuroprotective activities. In particular, a role in neurodegenerative disorders has been suggested for the I_2 receptor ligands 2-BFI and idazoxan, through inhibition of NMDAR-mediated intracellular calcium influx[32] or binding to MAO-B enzyme.[33,34] In contrast, molecules **9**, **10**, and **17** displayed strong protection against Aβ-mediated neuronal death by imidazoline I_2 receptor binding but with any significant affinity for NMADR and MAO-B (Figure 5). Altogether, the results reported in this work establish a key role for imidazoline I_2 receptors in Aβ-mediated neurotoxicity and AD pathogenesis.

This notwithstanding, it is worth stressing that translatability of these compounds into a potential efficacious human therapy is not straightforward from the in vitro results presented here. This is particularly important in the area of CNS diseases, as many promising in vitro agents have been ultimately shown to fail to recapitulate in vivo. Efforts toward optimizing the potency of the three active molecules identified on the I_2 receptor, addressing their selectivity across a wider panel of protein targets, and assessing their preclinical toxicity profile are currently underway in our laboratory. In addition, to have a better understanding of the exact role played by imidazoline receptors during in vivo AD progression and the potential scope of the compounds for in vivo neuroprotection, testing in animal models for AD would be required. In this regard, several transgenic mice have been developed in an attempt to mimic changes in the psychological and behavioral symptoms seen in AD patients.[35,36] Although none of them models the human pathology exactly, transgenic mice have become an useful tool to analyze molecular disease mechanisms and for testing therapeutic agents.[37]

AD is a complex multifactorial disease associated with multiple biological targets and pathways. The diversity of mechanisms of action offered by the therapeutic agents in use or under development for AD is a good reflection of this complexity. However, all of these agents focus primarily on improving the symptoms but not on blocking or even reversing the progression of the disease. The research presented here sheds new light into the molecular mechanisms involved in AD pathogenesis and points to interacting with the imidazoline I_2 receptor as a new therapeutic strategy for this fatal neurodegenerative disease.

EXPERIMENTAL SECTION

Virtual Chemical Screening and Target Profiling. In silico chemical screening against a catalogue of chemical providers composed of over 2 million molecules was performed using a similarity-based approach that relied on Memantine and MK-801 as reference structures to identify all commercially available molecules having similar feature-pair distributions as defined by Shannon entropy descriptors (SHED).[14]

In silico target profiling was later performed with PredictFX,[38] a similarity-based approach to target profiling that relies on the availability of data sources that contain chemical structures with information on the binding or functional activity to protein targets and the use of mathematical descriptors (namely, PHRAG, FPD, and SHED) to encode those chemical structures.[19] On this basis, the affinity of a compound for a given target is estimated by inverse distance weighting interpolation of the experimental affinities from all neighboring molecules found within a predetermined applicability domain.[19] The output returns a list of targets for which affinity is predicted for each molecule.

Compound Acquisition. Compounds **1**−**4**, **6**, **13**, and **14** were purchased from Specs, compounds **11**, **12**, and **15**−**17** were purchased from ChemDiv, compounds **7**, **9**, and **10** were purchased from Enamine, and compounds **5** and **8** were purchased from Asinex (Table S2 in the Supporting Information). The structures of all molecules were characterized and confirmed by the respective chemical providers prior to delivery, with guaranteed purity >95%.

Neuronal primary cultures. Primary cultures of mice hippocampal neurons (glial contamination <5%) were prepared from hippocampus of mouse OF1 embryos (E15.5) as described.[39] Cells were cultured onto poly-D-lysine-coated dishes in DMEM medium containing B27 supplement (Gibco-BRL). All animal procedures met the guidelines of European Community Directive and were approved by the PRBB ethical committee.

tPA Treatment and Detection of Erk1/2 Activation by ELISA Assays. For ELISA assays, hippocampal neurons were seeded at 10.000 cells/well in 96-multiwell plates (Nunc) coated with poly-L-Lys (SIGMA) and were cultured for 7 days. tPA (Actilyse, Boehringer Ingelheim) was added to the culture medium at 20 μg/mL for 1 h. Memantine, MK-801, or molecules **1**−**17** (30 μM) were added 4 h prior to tPA treatment.

After treatment, cells were fixed (methanol, −20 °C, 5 min) and ELISA (enzyme-linked immunosorbent assay) assays were performed to detect Erk1/2. Cells were washed with TBST (Tris buffer saline, 0.1% TritonX-100) and blocked with 5% normal horse serum in TBST for 1 h at 37 °C. Primary antibody anti phospho-Erk1/2 (Cell Signaling) or total Erk1/2 (Upstate) was added and incubated overnight at 4 °C. As a secondary antibody, alkaline phosphatase-conjugated anti-rabbit Ig (DAKO) was added for 1 h at 37 °C. After washing with TBST, 4-methylumbelliferyl phosphate (MPU, 1 mg/mL in 0.2 M triethanolamine, pH 8.5) was added as a substrate (30 min, RT). The fluorescence intensity was measured by a fluorescence microplate reader (Cytofluor 235, Millipore) at excitation/emission wavenlenghts of 360−460 nm. Cells incubated with substrate (MPU) alone or with the secondary antibody plus substrate were used as negative controls. Values were normalized to total Erk1/2. All assays were conducted in triplicate, and four independent experiments were performed for each compound.

Aβ-40 Treatment and Apoptosis TUNEL Detection. Primary hippocampal neurons were seeded at 100.000 cells/well in 24-well plates (Nunc) coated with poly-L-Lys (SIGMA) and were cultured for 7 days. Aβ-40 peptide [Amyloidβ Protein (1−40) trifluoroacetate salt, Bachem] was added to the medium at 20 μM for 72 h. Inhibitors (30 μM) were added 4 h prior to Aβ-40 treatment. Neurons with damaged DNA were detected using the terminal deoxynucleotidyl transferase-mediated dUTP nick-end labeling (TUNEL) detection kit (In Situ Cell Death Detection Kit, Roche) according to the manufacturer's manual. Briefly, cells were fixed with 4% paraformaldehyde in PBS (10 min, RT), permeabilized with 0.5% PBS-Triton, and incubated with labeling reaction mixture. Cells were subsequently stained with anti-NeuN (Neuronal nuclei) mouse antibody (Chemicon-Millipore) and a Cy3-labeled antimouse Ig secondary antibody (Jackson immunoresearch laboratories) to visualize neuronal nuclei. The TUNEL-positive cells (green) and cells with a small nucleus, high fluorescence intensity due to chromatin condensation or nuclear fragmentation were considered as apoptotic neurons. For cell counts, five random fields (about 60 cells/field) were observed per coverslip. Results were expressed as the percentage of apoptotic neurons relative to the total number of nuclei counted per coverslip. All experiments were conducted in duplicates, and four independent experiments were performed.

Statistical Analyses. All data from ELISA and TUNEL assays are shown as means ± SEMs for $n = 4$ experiments. Comparisons of groups were performed using two-tailed Student's t test. P values ≤ 0.05 were considered to be statistically significant.

In Vitro Pharmacology. The following list of in vitro binding assays was performed at Ricerca Biosciences (catalogue number in parentheses): the agonist/glutamate (232810), glycine (232910), phencyclidine (233000), and polyamine (234000) binding sites of NMDAR, 5-HT_{1A} (271110), 5-HT_{2A} (271650), 5-HT_{2C} (271800), D_2 (219600), M_3 (252810), M_4 (252910), M_5 (253010), DOP (260110), KOP (260210), MOP (260410), 5-HT_3 (271910), and SIGMAR (278110). The remaining in vitro binding assays were performed at Cerep (catalogue number in parentheses): α_2 nonselective (0297), MC4R (0420), I_1 (0642), I_2 (0081), AChE (0363), and MAO-B (3477).

ASSOCIATED CONTENT

Supporting Information

Full list of all 1758 virtual hits (Supplementary Table S1), the provider sources and original identifiers of the 17 compounds selected (Supplementary Table S2), and the dose−response curves of the binding interaction between compound **9** and the imidazoline I_1 receptor and compounds **9**, **10**, and **17** and the imidazoline I_2 receptor (Supplementary Figure S1). This material is available free of charge via the Internet at http://pubs.acs.org.

AUTHOR INFORMATION

Corresponding Author

*Tel: +34 93 3160550. Fax: +34 93 3160540. E-mail: jmestres@imim.es (J.M.). Tel: +34 93 3160428. Fax: +34 93 3160410. E-mail: pnavarro@imim.es (P.N.).

Author Contributions

J.M. and P.N. conceived and designed the study. E.G.-P. performed the computations for compound acquisition and target deconvolution. M.M. and D.P. performed all in vitro and cell-based experiments. J.M. and P.N. wrote the paper.

Notes

The authors declare the following competing financial interest(s): We are coinventors of two patents (Spanish patent numbers P200800876 and P200800877, deposited on March 28th, 2008) covering the use for Alzheimers disease of three of the molecules described in the manuscript.

ACKNOWLEDGMENTS

We are very grateful to Dr. Neus Martínez-Bosch for valuable help with statistical analysis. This work was supported by research grants SAF2005-00704 and PET2006_0514 from the Spanish Ministerio de Educación y Ciencia—Fondos Europeos de Desarrollo Regional (FEDER), PI080421 from the Instituto de Salud Carlos III—FEDER, BIO2011-26669 from the Ministerio de Ciencia e Innovación, and 2009SGR1409 from the Generalitat de Catalunya. Additional funding was provided

by IMADE, project no. PIE/739/2009, and by a collaborative project with Farmalider SA.

■ ABBREVIATIONS USED

2-BFI, 2-(2-benzofuranyl)-2-imidazoline; CNS, central nervous system; NMDAR, NMDA receptor; tPA, tissue plasminogen activator

■ REFERENCES

(1) Dhillon, A. S.; Hagan, S.; Rath, O.; Kolch, W. MAP kinase signalling pathways in cancer. *Oncogene* **2007**, *26*, 3279−3290.

(2) Harper, S. J.; Wilkie, N. MAPKs: New targets for neurodegeneration. *Expert Opin. Ther. Targets* **2003**, *7*, 187−200.

(3) Peng, S.; Zhang, Y.; Zhang, J.; Wang, H.; Ren, B. ERK in learning and memory: A review of recent research. *Int. J. Mol. Sci.* **2010**, *11*, 222−232.

(4) Webster, B.; Hansen, L.; Adame, A.; Crews, L.; Torrance, M.; Thal, L.; Masliah, E. Astroglial activation of extracellular-regulated kinase in early stages of Alzheimer disease. *J. Neuropathol. Exp. Neurol.* **2006**, *65*, 142−151.

(5) Dineley, K. T.; Westerman, M.; Bui, D.; Bell, K.; Ashe, K. H.; Sweatt, J. D. Beta-amyloid activates the mitogen-activated protein kinase cascade via hippocampal alpha7 nicotinic acetylcholine receptors: In vitro and in vivo mechanisms related to Alzheimer's disease. *J. Neurosci.* **2001**, *21*, 4125−4133.

(6) Medina, M. G.; Ledesma, M. D.; Dominguez, J. E.; Medina, M.; Zafra, D.; Alameda, F.; Dotti, C. G.; Navarro, P. Tissue plasminogen activator mediates amyloid-induced neurotoxicity via Erk1/2 activation. *EMBO J.* **2005**, *24*, 1706−1716.

(7) Cummings, J. L. Alzheimer's disease. *N. Engl. J. Med.* **2004**, *351*, 56−67.

(8) Walsh, D. M.; Selkoe, D. J. A beta oligomers—A decade of discovery. *J. Neurochem.* **2007**, *101*, 1172−1184.

(9) Jang, J. H.; Surh, Y. J. Beta-amyloid-induced apoptosis is associated with cyclooxygenase-2 up-regulation via the mitogen-activated protein kinase-NF-kappaB signaling pathway. *Free Radical Biol. Med.* **2005**, *38*, 1604−1613.

(10) Echeverria, V.; Ducatenzeiler, A.; Dowd, E.; Janne, J.; Grant, S. M.; Szyf, M.; Wandosell, F.; Avila, J.; Grimm, H.; Dunnett, S. B.; Hartmann, T.; Alhonen, L.; Cuello, A. C. Altered mitogen-activated protein kinase signaling, tau hyperphosphorylation and mild spatial learning dysfunction in transgenic rats expressing the beta-amyloid peptide intracellularly in hippocampal and cortical neurons. *Neuroscience* **2004**, *129*, 583−592.

(11) Collen, D.; Lijnen, H. R. Tissue-type plasminogen activator: a historical perspective and personal account. *J. Thromb. Haemostasis* **2004**, *2*, 541−546.

(12) Wong, E. H.; Kemp, J. A.; Priestley, T.; Knight, A. R.; Woodruff, G. N.; Iversen, L. L. The anticonvulsant MK-801 is a potent N-methyl-D-aspartate antagonist. *Proc. Natl. Acad. Sci. U.S.A.* **1986**, *83*, 7104−7108.

(13) Parsons, C. G.; Gruner, R.; Rozental, J.; Millar, J.; Lodge, D. Patch clamp studies on the kinetics and selectivity of N-methyl-D-aspartate receptor antagonism by memantine (1-amino-3,5-dimethyladamantan). *Neuropharmacology* **1993**, *32*, 1337−1350.

(14) Gregori-Puigjane, E.; Mestres, J. SHED: Shannon entropy descriptors from topological feature distributions. *J. Chem. Inf. Model.* **2006**, *46*, 1615−1622.

(15) Gallastegui, E.; Marshall, B.; Vidal, D.; Sanchez-Duffhues, G.; Collado, J. A.; Alvarez-Fernandez, C.; Luque, N.; Terme, J. M.; Gatell, J. M.; Sanchez-Palomino, S.; Munoz, E.; Mestres, J.; Verdin, E.; Jordan, A. Combination of biological screening in a cellular model of viral latency and virtual screening identifies novel compounds that reactivate HIV-1. *J. Virol.* **2012**, *86*, 3795−3808.

(16) Gregori-Puigjané, E.; Garriga-Sust, R.; Mestres, J. Indexing molecules with chemical graph identifiers. *J. Comput. Chem.* **2011**, *32*, 2638−2646.

(17) Rapoport, M.; Ferreira, A. PD98059 prevents neurite degeneration induced by fibrillar beta-amyloid in mature hippocampal neurons. *J. Neurochem.* **2000**, *74*, 125−133.

(18) Youdim, M. B.; Buccafusco, J. J. CNS Targets for multi-functional drugs in the treatment of Alzheimer's and Parkinson's diseases. *J. Neural Transm.* **2005**, *112*, 519−537.

(19) Laggner, C.; Kokel, D.; Setola, V.; Tolia, A.; Lin, H.; Irwin, J. J.; Keiser, M. J.; Cheung, C. Y.; Minor, D. L., Jr.; Roth, B. L.; Peterson, R. T.; Shoichet, B. K. Chemical informatics and target identification in a zebrafish phenotypic screen. *Nat. Chem. Biol.* **2011**, *8*, 144−146.

(20) Vidal, D.; Mestres, J. In silico receptorome screening of antipsychotic drugs. *Mol. Inf.* **2010**, *29*, 543−551.

(21) Flachner, B.; Lorincz, Z.; Carotti, A.; Nicolotti, O.; Kuchipudi, P.; Remez, N.; Sanz, F.; Tovari, J.; Szabo, M. J.; Bertok, B.; Cseh, S.; Mestres, J.; Dorman, G. A chemocentric approach to the identification of cancer targets. *PLoS One* **2012**, *7*, e35582.

(22) Areias, F. M.; Brea, J.; Gregori-Puigjane, E.; Zaki, M. E.; Carvalho, M. A.; Dominguez, E.; Gutierrez-de-Teran, H.; Proenca, M. F.; Loza, M. I.; Mestres, J. In silico directed chemical probing of the adenosine receptor family. *Bioorg. Med. Chem.* **2010**, *18*, 3043−3052.

(23) Mestres, J.; Seifert, S. A.; Oprea, T. I. Linking pharmacology to clinical reports: Cyclobenzaprine and its possible association with serotonin syndrome. *Clin. Pharmacol. Ther.* **2011**, *90*, 662−665.

(24) Sun, Z.; Chang, C. H.; Ernsberger, P. Identification of IRAS/Nischarin as an I1-imidazoline receptor in PC12 rat pheochromocytoma cells. *J. Neurochem.* **2007**, *101*, 99−108.

(25) Garcia-Sevilla, J. A.; Escriba, P. V.; Walzer, C.; Bouras, C.; Guimon, J. Imidazoline receptor proteins in brains of patients with Alzheimer's disease. *Neurosci. Lett.* **1998**, *247*, 95−98.

(26) Ferrari, F.; Fiorentino, S.; Mennuni, L.; Garofalo, P.; Letari, O.; Mandelli, S.; Giordani, A.; Lanza, M.; Caselli, G. Analgesic efficacy of CR4056, a novel imidazoline-2 receptor ligand, in rat models of inflammatory and neuropathic pain. *J. Pain Res.* **2011**, *4*, 111−125.

(27) Dardonville, C.; Fernandez-Fernandez, C.; Gibbons, S. L.; Ryan, G. J.; Jagerovic, N.; Gabilondo, A. M.; Meana, J. J.; Callado, L. F. Synthesis and pharmacological studies of new hybrid derivatives of fentanyl active at the mu-opioid receptor and I2-imidazoline binding sites. *Bioorg. Med. Chem.* **2006**, *14*, 6570−6580.

(28) Treder, A. P.; Andruszkiewicz, R.; Zgoda, W.; Walkowiak, A.; Ford, C.; Hudson, A. L. New imidazoline/alpha(2)-adrenoceptors affecting compounds-4(5)-(2-aminoethyl)imidazoline (dihydrohistamine) derivatives. Synthesis and receptor affinity studies. *Bioorg. Med. Chem.* **2011**, *19*, 156−167.

(29) Tomassoli, I.; Ismaili, L.; Pudlo, M.; de Los, R. C.; Soriano, E.; Colmena, I.; Gandia, L.; Rivas, L.; Samadi, A.; Marco-Contelles, J.; Refouvelet, B. Synthesis, biological assessment and molecular modeling of new dihydroquinoline-3-carboxamides and dihydroquinoline-3-carbohydrazide derivatives as cholinesterase inhibitors, and Ca channel antagonists. *Eur. J. Med. Chem.* **2011**, *46*, 1−10.

(30) Bolea, I.; Juarez-Jimenez, J.; de Los, R. C.; Chioua, M.; Pouplana, R.; Luque, F. J.; Unzeta, M.; Marco-Contelles, J.; Samadi, A. Synthesis, biological evaluation, and molecular modeling of donepezil and N-[(5-(benzyloxy)-1-methyl-1H-indol-2-yl)methyl]-N-methylprop-2-yn-1-amine hybrids as new multipotent cholinesterase/monoamine oxidase inhibitors for the treatment of Alzheimer's disease. *J. Med. Chem.* **2011**, *54*, 8251−8270.

(31) National Institute for Health and Clinical Excellence. Donezepil, galantamine, rivastigmine and memantine for the treatment of Alzheimer's disease. NICE technology appraisal guidance 217, 2011 (http://guidance.nice.org.uk/TA217).

(32) Jiang, S. X.; Zheng, R. Y.; Zeng, J. Q.; Li, X. L.; Han, Z.; Hou, S. T. Reversible inhibition of intracellular calcium influx through NMDA receptors by imidazoline I(2) receptor antagonists. *Eur. J. Pharmacol.* **2010**, *629*, 12−19.

(33) Soto, J.; Ulibarri, I.; Jauregui, J. V.; Ballesteros, J.; Meana, J. J. Dissociation between I2-imidazoline receptors and MAO-B activity in platelets of patients with Alzheimer's type dementia. *J. Psychiatr. Res.* **1999**, *33*, 251−257.

(34) McDonald, G. R.; Olivieri, A.; Ramsay, R. R.; Holt, A. On the formation and nature of the imidazoline I2 binding site on human monoamine oxidase-B. *Pharmacol. Res.* **2010**, *62*, 475−488.
(35) Spires, T. L.; Hyman, B. T. Transgenic models of Alzheimer's disease: Learning form animals. *NeuroRX* **2005**, *2*, 423−437.
(36) R. Lalonde, R.; Fukuchi, K.; Strazielle, C. APP transgenic mice for modelling behavioural and psychological symptoms of dementia (BPSD). *Neurosci. Biobehav. Rev.* **2012**, *36*, 1357−1375.
(37) Duff, K.; Suleman, F. Transgenic mouse models of Alzheimer's disease: how useful have they been for therapeutic development? *Briefings Funct. Genomics Proteomics* **2004**, *3*, 47−59.
(38) Chemotargets SL. http://www.certara.com/products/predictfx/, 2012.
(39) Goslin, K.; Banker, G. *Culturing Nerve Cells*; MIT Press: Cambridge, MA, 1991; pp 251−281.